

PRODUCTION OF MASSIVE LEPTON PAIRS*

M. Duong-van** and R. Blankenbecler

Stanford Linear Accelerator Center
Stanford University, Stanford, California 94305

ABSTRACT

Some general criteria for the validity of the hard scattering expansion are discussed and applied to the production of massive lepton pairs. Problems and inconsistencies in adding transverse momentum to the quark distribution are described in detail. Tests to differentiate between different sources for the transverse momentum of the photon and different models are given. Sample numerical predictions of the meson-quark model (which in a previous paper was shown to fit proton beam data) are presented for meson beam processes. Further tests of the model are described, and a simple universal transverse momentum distribution is given that is expected to hold for all beam particles.

(Submitted to Phys. Rev.)

*Supported by the Department of Energy.

**Present address: University of California, Los Alamos Scientific Laboratory,
Los Alamos, New Mexico 87544.

I. INTRODUCTION

In a previous paper,¹ a simple model, the meson-quark, or M-q model, for the production of massive lepton pairs was described and numerically compared to proton beam data. The model was shown to reproduce the Drell-Yan model² (D-Y) predictions for the pair mass distributions (integrated over transverse momentum Q_T which are dominated by the region $Q_T \ll Q$). The M-q model also agrees with the constituent interchange model³ for $Q_T \gg Q$ and in particular reproduces the predictions for real photon production at large Q_T . The model gave a broad transverse momentum spectrum in contrast to the assumptions made in the original Drell-Yan model. It also allowed two independent methods of normalizing the predicted yield, both of which agreed reasonably well with the data. One method was to fit the measured antiquark distribution functions; the other was to fit the measured rate for large p_T production of mesons.

In this note we wish to do two things. One is to review some general aspects of the hard scattering model expansion, and point out several errors in principle made in some treatments of the D-Y process (and in large p_T hadron production as well). The second is to discuss a few useful general predictions of the M-q model and to present some numerical predictions for pion means. The basic hard scattering model diagram for the production of a massive pair is given in Fig. 1a. The total yield is a sum over intermediate states a and b (and the final state d). These terms must be incoherent—and this requires, for example, that a beam fragment in one term (in the sum over a and b) not be allowed to end up in the same part of phase space as an identical fragment from the central process of another term in the sum (all other particles being the same). This is a difficult requirement to enforce with mathematical precision. Clearly one can

easily make a mistake in this regard if large momentum transfer scattering is allowed in both the beam or target vertex (or structure) function and the central scattering process. Simply adding a broad transverse momentum to the beam fragmentation function can lead to double counting (as well as trouble with gauge invariance in the present reaction). To avoid this problem we shall insist that all large momentum transfer scatterings occur in the central process only. In this way we can avoid double counting and coherence problems but yet can include all possible diagrams. Let us turn immediately to a more specific discussion of the general criteria for the validity of the hard scattering expansion.

II. THE HARD SCATTERING MODEL

The hard scattering model provides a simple and appealing picture of scattering processes. It has been some time since the hard scattering expansion (or the impulse approximation) was derived and it seems appropriate at this time to review the basic assumptions used. This is particularly important since, as we shall see, it is quite easy to violate these assumptions. By adding on perfectly reasonable features to the first term in the expansion, it is very easy to derive nonsense.

Of particular interest to us is the production of massive lepton pairs via a virtual photon in which gauge invariance pushes us towards a correct treatment. The general features that will be discussed here are relevant, however, even for large p_T production of hadrons. The hard scattering expansion for the production of a lepton pair of four-momentum Q is conventionally written as (see Fig. 1a)

$$Q^4 \frac{d\sigma}{dQ^4}(AB \rightarrow \ell^+ \ell^- X) = \sum_{a, b, d} \int dx d^2k_T dy d^2\ell_T G_{a/A}(x, k_T) G_{b/B}(y, \ell_T) Q^4 \frac{d\sigma}{dQ^4}(ab \rightarrow \ell^+ \ell^- d; s', t', u'; Q^2) \quad (1)$$

where, if k_T and l_T are not too large,

$$\begin{aligned} s' &= xys \\ t' &= xt + (1-x)Q^2 \\ u' &= yu + (1-y)Q^2 \end{aligned} \quad (2)$$

Certain kinematic factors that are approximately unity if a and b are not too far off-shell have been dropped in the above.⁴

The sum over the intermediate and final states must be chosen so that Eq. (1) is a sum over incoherent final states. This means that the simplest way to classify the terms is according to the final state configuration of particles, not the possible intermediate states that can contribute. The sum over a, b, and d must be chosen with the final state configurations in mind. For example, this means that one particular Feynman graph contributes to several terms in the sum depending upon the disposition of the final state particles, that is which particular particle (or particles) is recoiling against the large Q_T of the photon in our example. This is described pictorially in Fig. 2. The three terms illustrate the hard scattering expansion and they are identified according to whether α , β , or d are recoiling against the detected particle c. Note that the intermediate particles, a+b, b, and a, respectively, are then always near shell (their masses are limited, not of order $|c_T|$).

Let us now turn to the problem of the incoherence of various contributions to the D-Y process. Consider the two diagrams in Fig. 3 which correspond to $a=\bar{q}$, $b=q$, and $b=(qq)$, respectively. The first diagram is the natural one to add to the Drell-Yan theory in order to produce large Q_T pairs. The large transverse momentum of the pair arises from the wave function or structure function $G_{q/p}(y, l_T)$. However, this is an incorrect treatment since the second $b=(qq)$ term is coherent with the first and is even of the same order. It is simplest to

treat these two terms together and to include them both in the second diagram. These combined contributions should perhaps be drawn as in Fig. 4 which emphasizes their coherence and also the fact that the existence of both terms are demanded by gauge invariance. In this form they can be described as an initial and a final state interaction, respectively. From the relevant quark's point of view, they are the direct and crossed graph for the process $\text{glue} + \text{quark} \rightarrow \text{photon} + \text{quark}$. At large Q_T , one finds that these two terms cancel to leading order. This feature was described in terms of the M-q model¹ but is a general phenomena.

That this is not an unexpected feature of initial and final state interactions can be seen by considering the theorem derived in potential scattering by Amado and Woloshyn.⁵ They proved that the term with the leading behavior of the wave function at large relative momentum actually cancels in a general class of breakup reactions. This cancellation is due essentially to the orthogonality of the bound and (ingoing) scattering states and is therefore expected to be a very general phenomena.

We have seen therefore that simply adding a large k_T spectrum to the initial state quarks and then using the Drell-Yan formula is incorrect in principle.⁶ This should come as no surprise since D-Y stated in their original paper² that their model was not gauge invariant if large transverse momenta were allowed. It is easy to see that if an intermediate quark carries a large k_T , its (mass)² is of order $(-k_T^2/(1-x))$. Thus it is not possible to make such a contribution gauge invariant to this order unless the photon is attached to both ends of this far off-shell propagator. This leads us naturally to the initial and final state interaction effects described earlier. One way to avoid troubles here is to demand that the intermediate particles a and b remain near their respective mass shells

and hence that they not carry a large transverse momentum. This forces all large momentum transfers to occur in the central process. This in turn allows the photon to be attached in all necessary orderings to insure gauge invariance.

Let us now turn to the M-q model which is one of the simplest ways to guarantee that the criteria described before are met, but is certainly not the only way. Among the interesting features of the model to be kept in mind is the fact that it allows two independent methods of normalization of the rate.

III. THE M-q MODEL

In Ref. 1, the cross section for meson + quark $\rightarrow \ell^+ \ell^-$ + quark, was shown to be (see Fig. 1b)

$$Q^4 \frac{d\sigma}{d^4Q} (Mq \rightarrow \ell^+ \ell^- q) = \frac{1}{6\pi^2} \alpha^2 h^2 \delta(s+t+u-Q^2-2M^2) \Sigma(s, t, u; Q^2) \quad (3)$$

where

$$\begin{aligned} s\Sigma(s, t, u; Q^2) &= \frac{\lambda^2(u, Q^2, M^2)}{(M^2-u)^2} + \frac{\lambda^2(s, Q^2, M^2)}{(M^2-s)^2} \\ &+ \frac{2}{(s-M^2)(M^2-u)} \left[2Q^2(s-Q^2+u) + (s-Q^2-M^2)(u-Q^2-M^2) \right] \end{aligned}$$

and

$$\lambda^2(a, b, c) = a^2 + b^2 + c^2 - 2(ab + bc + ca) \quad .$$

The full cross section of a beam particle A on a target particle B is then

$$Q^4 \frac{d\sigma}{d^4Q} (AB \rightarrow \ell^+ \ell^- X) = \sum_{a, b, d} \int dx dy G_{a/A}(x) G_{b/B}(y) Q^4 \frac{d\sigma}{d^4Q} (ab \rightarrow \ell^+ \ell^- d; s't'u'; Q^2) \quad (4)$$

and the k_T and l_T distributions were assumed narrow to satisfy the incoherence criteria discussed in the previous section.⁹ These dominant contributions are illustrated in Fig. 5a, b and therefore the intermediate states a and b take on the values $a=q, \bar{q}$, $b=M$ and $a=M$, $b=q$. In the case that the beam is a meson itself, the former contribution contains the so-called direct scattering term shown in Fig. 5c, and for which $G_{M/M}(x) = \delta(1-x)$. These are the three dominant contributions to the pair yield in our model. They can be shown to correspond respectively to sea-valence, valence-sea, and valence-valence scattering in the D-Y language.

The large Q_T^2 and Q^2 distributions can be extracted from the above formulas by writing $xG_{a/A}(x) \propto (1-x)^{g_a}$, and similarly for b/B . By manipulations similar to those used to extract the large transverse momentum behavior in hard scattering models (see Ref. 3), but which are more involved because both Q^2 and Q_T^2 are large, it is possible from Eqs. (3) and (4) to derive the form

$$Q^4 \frac{d\sigma}{d^4Q} (AB \rightarrow l^+ l^- X) \cong K(Q_T^2, Q^2) \epsilon^F J(\epsilon, x_F) \quad (5)$$

where

$$K(Q_T^2, Q^2) \equiv \left(1 + \frac{Q_T^2}{\mu^2}\right)^{-2} \left(1 + \frac{Q_T^2}{\mu^2 + dQ^2}\right)^{-1}, \quad (6)$$

where μ is a mass parameter related to internal masses in the model, d is a constant ($d \approx 1$), J is slowly varying for small ϵ , and $F = 1 + g_a + g_b$. This is a universal characterization of the Q_T distribution for all beam particles (since μ and d are the same). Finally

$$\epsilon = \frac{M^2}{s} = 1 - \frac{t+u}{s} - \frac{Q^2}{s}, \quad (7)$$

where \mathcal{M} is the total missing mass with respect to the photon (hadron masses were neglected in the above kinematics). This form can be used to parametrize the detailed numerical calculation given in Ref. 1, and may prove useful in fitting data. After integrating over Q_T^2 , the factors $\langle \epsilon^F J(\epsilon, x_F) \rangle$ are simply related to the folding of structure functions in the Drell-Yan formula. The explicit ϵ^F factor characterizes the threshold behavior. After integrating over x_F and Q_T^2 , which adds an extra factor of ϵ^2 , the threshold behavior for the mass distribution $d\sigma/dQ^2$ is ϵ^{F+2} . For D-Y, this final power is 11 for pp scattering and 5 for πp scattering if one uses the dimensional counting predictions for the structure functions.¹⁰ For the meson-quark scattering case, $F=9$ and 3, respectively (again using dimensional counting), hence the final ϵ power is the same in the two cases. A more detailed discussion of the connection between the meson-quark model and the D-Y model was given in Ref. 1.

The above approximate form has the behavior Q_T^{-4} for $Q_T \ll Q$, and Q_T^{-6} for $Q_T \gg Q$. This latter behavior is in agreement with the dimensional counting rules for inverse photoproduction of real photons.¹⁰ It is easy to compute the average transverse momentum of the pair, $\langle Q_T \rangle$, in the limit of large energies. Neglecting the dependence of ϵ on Q_T (this dependence reduces the expected average transverse momentum), the result is

$$\langle Q_T \rangle = \frac{\pi\mu}{2} \frac{\left[\left(1 + \frac{dQ^2}{\mu^2} \right)^{1/2} - 1 \right]^2}{\left[\frac{dQ^2}{\mu^2} - \ln \left(1 + \frac{dQ^2}{\mu^2} \right) \right]} \quad (8)$$

Therefore $\langle Q_T \rangle$ has the limiting values

$$\begin{aligned} \langle Q_T \rangle &\cong \frac{\pi}{4} \mu & Q \ll \mu \\ &\cong \frac{\pi}{2} \mu (1 - 2\mu/\sqrt{d} Q) & Q \gg \mu \end{aligned} \quad (9)$$

An increase in $\langle Q_T \rangle$ as a function of Q has probably been observed in p-p collisions but unfortunately the most relevant experiments are at different values of x_F . Finally, we note that in the M-q model, the same value of μ and the same function $K(Q_T^2, Q^2)$ should describe lepton pair production for all incident beams. The only differences expected in the Q_T distributions are due to the small effects of the ϵ^F term and the differing values of F .

Now consider $\pi^\pm p$ scattering. The direct process (D) has $F=3$ which reflects the threshold behavior of the proton structure function, as illustrated in Fig. 5c. The process in which the intermediate meson arises from the beam meson (M) has $F=7$ as is clear from Fig. 5b. Finally, the process in which the intermediate meson arises from the target nucleon (N) also has $F=7$, see Fig. 5a. Using the above notation, the cross section for π^\pm for an isoscalar target can be characterized for ϵ not near one by the forms (detailed numerics will be given in a later section)

$$\begin{aligned} Q^4 \frac{d\sigma}{dQ^4}(\pi^-) &\simeq K(Q_T^2, Q^2) \left[4D\epsilon^3 + (M+N)\epsilon^7 \right] \\ Q^4 \frac{d}{dQ^4}(\pi^+) &\simeq K(Q_T^2, Q^2) \left[D\epsilon^3 + (M+N)\epsilon^7 \right], \end{aligned} \tag{10}$$

where the 4/1 ratio of the first terms reflect the square of the charge of the d and u quarks. Now as x_F increases, ϵ decreases, and eventually, a 4/1 ratio should be observed. This is a well known prediction for the valence contribution of the D-Y model. The M and N term correspond to scattering from the sea in the D-Y model.

However, we also see that in the model under discussion, a similar limiting behavior holds at very large Q_T . Now ϵ also decreases as Q_T increases, hence for very large transverse momenta a limiting 4/1 ratio should also be observed

no matter what the ratio is for small Q_T . In general, for kinematic points very far from the origin of the Peyrou plot, the ratio should be 4/1 for any value of the center of mass scattering angle. As Q increases, the transition moves inward (as does the edge of the plot) and will eventually reach the origin. This general behavior will be illustrated in the sample calculation to be given in a later section.

IV. TESTS FOR SOURCES OF LARGE Q_T

In this section we shall discuss possible sources for the observed large $\langle Q_T \rangle$ (even though some of them have to be modified in order to be consistent with the hard scattering expansion as discussed in Section II) and experimental tests to differentiate between them.

The M-q model and the model of Kinoshita *et al.*,¹¹ and Fontannaz¹² can best be described by saying that a hard scattering is the source of the large Q_T . Other models had added a broad k_T distribution to the valence quarks⁷ and others to the sea.⁸ The asymptotic freedom models are in this latter category since in order to find a more point-like quark, one must look further down the cascade chain,¹³ and this we classify as the sea. These models also assume that there is no difficulty in continuing from a space-like Q^2 to a time-like Q^2 in the running coupling constant, and we shall make the same smoothness assumption. However if there are large scale collective excitations in the theory, as one might expect from either the strong coupling in this regime (that is, confinement) or the effects of instantons, the behavior of the coupling at small Q^2 or large distances may be nonobvious and the continuation nontrivial.

Now two simple tests will be described. The first involves a comparison of $\langle Q_T \rangle$ for pp and $\pi^\pm p$ reactions. As discussed in the previous section, scattering models predict that there will be no difference between these different beams

(except for the small effects of the ϵ dependence). This is not the case for the valence and sea models. Instead of comparing the yield from π^+ and π^- beams directly, it is more convenient for obvious reasons to define the following linear combination of cross sections for an isoscalar target:

$$\begin{aligned}\pi_{\text{val}} &\equiv \frac{1}{3}(\pi^- - \pi^+) \\ \pi_{\text{sea}} &\equiv \frac{1}{3}(4\pi^+ - \pi^-) \quad .\end{aligned}\tag{11}$$

In the first combination, π_{val} , the sea of the mesons should cancel, so this cross section should be dominated by the $(\text{val})_{\pi} \times (\text{val})_p$ terms (in the D-Y model language). The second, π_{sea} , should be dominated by the sea of the meson and the valence of the proton. The expected relative values of $\langle Q_T \rangle$ for these three cross sections on an isoscalar target at a moderate Q value are shown in Table I for a valence and a sea source. The distinguishing characteristic between the various models is clear, namely π_{val} , as well as a consistency check between the proton beam and π_{sea} .

The second test of the models involves a study of the Q_T distribution for π^- and π^+ beams on an isoscalar target. For a fixed (moderate) Q value, one expects the distribution to be essentially parallel as illustrated in Fig. 6a (they eventually should become 4/1 at a very large Q_T where phase space controls the situation, i. e., ϵ is very small). If a broad valence distribution is the source of the Q_T , the distributions should quickly diverge to a 4/1 ratio as shown in Fig. 6b. However, if a broad sea is the source, then the curves should converge at large Q_T as in Fig. 6c.

V. NUMERICAL RESULTS

The expected Q_T distribution Eq. (5) is compared to the data of Hom et al. in Fig. 7 for the values $d=1$ and $\mu=0.9$ (GeV). These values also reproduce the

exact theoretical distributions given in Ref. 1 quite well. The dependence of $\langle Q_T \rangle$ on Q given by Eq. (8) is given in Fig. 8 and compared to the data of Hom et al.,¹⁴ Kluberg et al.,¹⁵ and Anderson et al.¹⁶ (Note—these latter points are measured at different energies and at forward x_F values. This increases the effect of the ϵ^F term and changes the expected $\langle Q_T \rangle$.) Finally, we note that the new values of $\langle Q_T \rangle$ from Hom et al. are much closer to the prediction made in Ref. 1 (see Fig. 8 therein) than their preliminary values.

The detailed numerical predictions of Eq. (4) are given for π^\pm beams in Figs. 9 and 10. The only unknown constant is the magnitude of $G_{M/\pi}$, which determine the magnitude of the M, meson, term. All other constants come from the fit of Ref. 1. In Fig. 9, the predicted Q_T distributions for π^\pm are compared with each other and with the available data on π^+ by Anderson et al.¹⁶ for $0.15 < x_F < 1$ and $1.13 < Q < 2$. The D^\pm , or direct, terms are shown as well as the N, nucleon, term. The M-term is negligible for $x_F > 0$. One sees that the curves are essentially parallel, and slowly start to diverge at large Q_T . They will eventually reach a 4/1 ratio at very large Q_T .

The predicted x_F distribution for the π^\pm beams are extremely interesting and are given in Fig. 10 for the same (low) Q range. The data points are the π^+ data from Anderson et al.¹⁶ There are several features of this prediction which are unexpected and can be used to test the M-q model. Note that the D term, which corresponds to the D-Y (val \times val) term, dominates for sufficiently forward x_F and will eventually lead to the expected 4/1 ratio. For negative x_F , however, the M-term dominates since the most important term is the u-pole, and this should lead to an equality of the π^+ and π^- cross sections. The value of the x_F required for this equality becomes more negative as Q increases. A

detailed experimental comparison of π^+ and π^- for a wide range of x_F as a function of Q is very important for testing models of massive lepton pair production.

VI. CONCLUSION

A review of some of the criteria required for the validity of the hard scattering expansion was given with emphasis on the problem of the addition of transverse momenta to the quarks, and to gauge invariance. Several experimental tests to determine the source of large Q_T lepton pairs were described.

Detailed numerical predictions were given in the text for meson beams in the M-q model. This model has been shown to provide a reasonable fit to both pion and proton beam production of massive lepton pairs. Further tests were described. The predictions of the model reduce to those of the Drell-Yan model for $Q_T \ll Q$, but it also provides a natural explanation of the broad transverse momentum distributions observed. For $Q_T \gg Q$, it agrees with the predictions of the CIM model and dimensional counting.¹⁷ It should join smoothly on the real photon production ($Q=0$) at large Q_T and the parameters (μ and normalization) should be the same. In this model, the dilepton transverse momentum should follow a definite but simple universal power law falloff (Eq. (5)). This prediction, made in Ref. 1, is consistent with the recent high mass, high statistics experiment of Ref. 14.

One further prediction of this model is that the ratio of massive lepton pairs with transverse momentum Q_T to pions with Q_T should behave as

$$r = \frac{Q^4 \frac{d\sigma}{dQ^4} (AB \rightarrow \ell^+ \ell^- X)}{Q_0 \frac{d\sigma}{d^3Q} (AB \rightarrow \pi X)} \propto \left(1 + \frac{Q_T^2}{\mu^2}\right)^2 \left(1 + \frac{Q_T^2}{\mu^2 + dQ^2}\right)^{-1}$$

for large Q_T and Q and $s \gg Q_T^2 + Q^2$. An experimental confirmation of the power behavior $r \sim Q_T^4$ for $Q_T \ll Q$, and $r \sim Q_T^2$ for $Q_T \gg Q$ would be strong evidence

for the meson-quark model. Predictions and interesting features of the x_F distribution of lepton pairs from π^\pm beams were also given and these also remain to be tested.

Acknowledgements

We wish to thank S. J. Brodsky, W. Caswell, R. Horgan, and K. Vasavada for helpful conversations.

REFERENCES

1. M. Duong-van, K. V. Vasavada, and R. Blankenbecler, Stanford Linear Accelerator Center preprint SLAC-PUB-1882 (1977) (to be pub. in Phys. Rev.).
2. S. D. Drell and T.-M. Yan, Phys. Rev. Letters 25, 316 (1970); Ann. Phys. 6b, 578 (1971).
3. R. Blankenbecler, S. J. Brodsky, and J. F. Gunion, Phys. Rev. D 6, 2652 (1972). See also D. Sivers, S. J. Brodsky, and R. Blankenbecler, Phys. Reports 23C, No. 1 (1976).
4. For some details of the derivation of this formula in modern notation, see the Appendix of the second article in Ref. 3.
5. R. D. Amado and R. M. Woloshyn, IAS preprint 77-0374 (1977).
6. We find it very surprising that such a simple and appealing physical picture is inconsistent. Other authors who should share this surprise are found in Refs. 7 and 8. It is good to be occasionally reminded that quantum mechanics is different from classical mechanics.
7. P. Landshoff, preprint DAMTP 76/23 (1976). J. F. Gunion, University of California, Davis preprint (1976). D. Soper, Phys. Rev. Letters 38, 461 (1971).
8. J. Kogut, Phys. Letters 65B, 377 (1976). J. Kogut and J. Shigemitsu, Cornell preprint (1977). C. S. Lam and T.-M. Yan, CLNS preprint (1977).
9. The effects of initial state transverse momentum fluctuations have been studied in considerable detail by S. J. Brodsky, W. Caswell, and R. Horgan (to be published).
10. R. Blankenbecler and S. J. Brodsky, Phys. Rev. D 16, 2973 (1974).
11. K. Kinoshita, Y. Kinoshita, J. Cleymans, and B. Petersson, Bielefeld preprint (1977); Phys. Letters 68B, 355 (1977).

12. M. Fontannaz, Phys. Rev. D 14, 3127 (1976).
13. J. Kogut and L. Susskind, Phys. Rev. D 9, 697, 3391 (1974).
14. L. Lederman, "Observation of a Dimuon Resonance at 9.5 GeV," 1977 International Symposium on Lepton and Photon Interactions at High Energies, Congress Centrum Hamburg, August 25-31, 1977.
15. L. Kluberg et al., Phys. Rev. Letters 37, 1451 (1976).
16. K. J. Anderson et al., Phys. Rev. Letters 37, 799 (1976).
17. As expected the spin of the quarks has no effect on the final photon distribution, but it will affect the angular dependence of correlation measurements (see Ref. 1). An explicit calculation of the effects of spin has been carried out by C. M. Debeau and D. Silverman, University of California, Irvine preprint UCI 77-28 (1977).

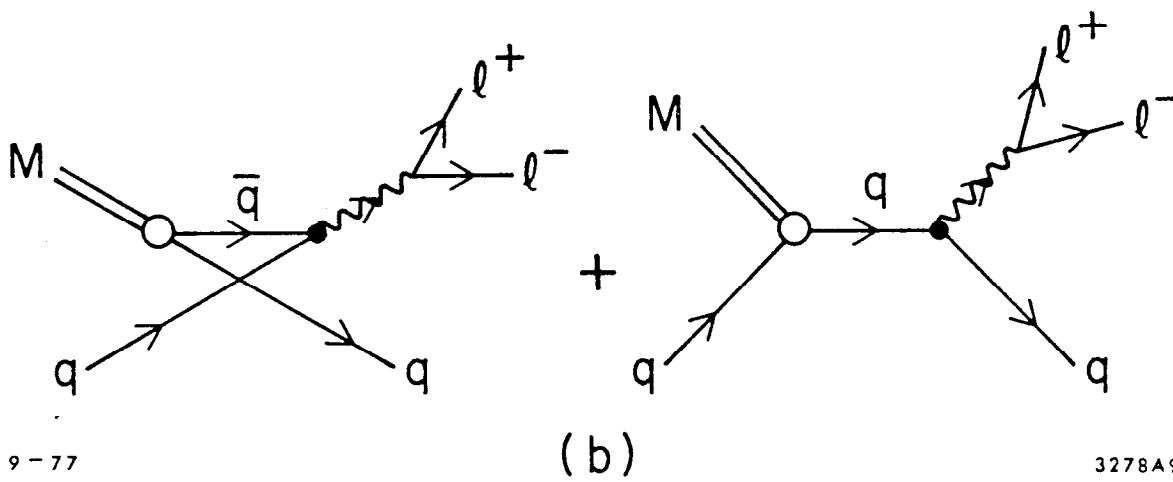
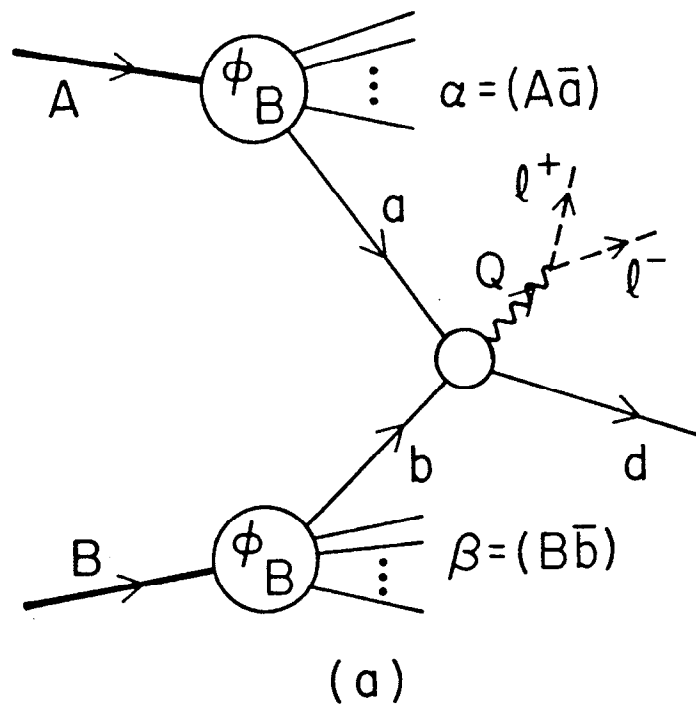
TABLE I

$\langle Q_T \rangle$ For Different Sources

Beam	Dominant	Expected $\langle Q_T \rangle$ if due to		
	D-Y Label	Scattering	Valence	Sea
p	sea \times val	large	large	large
π_{val}	val \times val	large	$\sqrt{2} \times$ large	small
π_{sea}	sea \times val	large	large	large

FIGURE CAPTIONS

1. (a) A general term in the hard scattering expansion, and (b) the dominant graphs in the basic process $Mq \rightarrow \ell^+ \ell^- q$. The Drell-Yan process is contained in the first (u-pole) term.
2. The decomposition of one Feynman graph into several hard scattering graphs classified according to the final state configurations.
3. An illustration of the final state coherence of two superficially different terms.
4. A redrawing of Fig. 3 showing the two attachment points of the photon as required by gauge invariance.
5. An illustration of the three dominant terms in the meson-proton reaction. The labels N, M and D denote the source of the intermediate meson.
6. The expected trends of the Q_T distributions for π^- and π^+ beams for different sources of the transverse momentum of the photon.
7. The approximate Q_T distribution derived in the text (Eq. (6)) for $d=1$ and $\mu=0.9$ and compared to the data of Ref. 14 for proton beams.
8. The predicted $\langle Q_T \rangle$ of the text, Eq. (8), compared to the data of Refs. 14, 15, and 16.
9. The predicted Q_T distribution using exact numerical integration for charge pion beams and the kinematics as shown. The experimental points are fit π^+ beam, Ref. 16.
10. The predicted x_F distributions for charged pion beams showing the D^\pm , M, and N contributions. The data points are for π^+ beams at 150 GeV, Ref. 16.



9-77

3278A9

Fig. 1

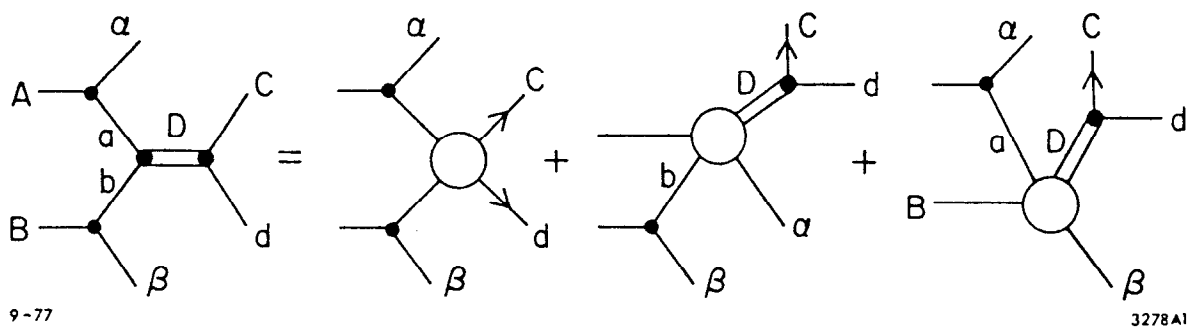
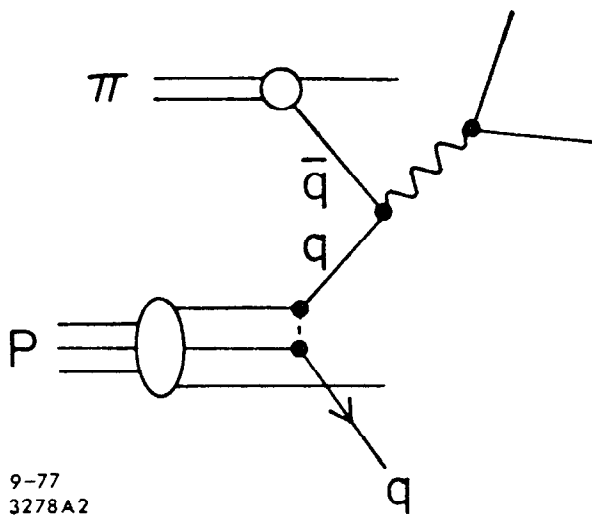


Fig. 2



9-77
3278A2

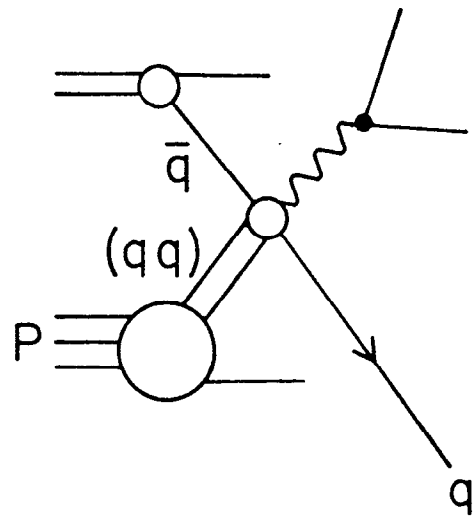


Fig. 3

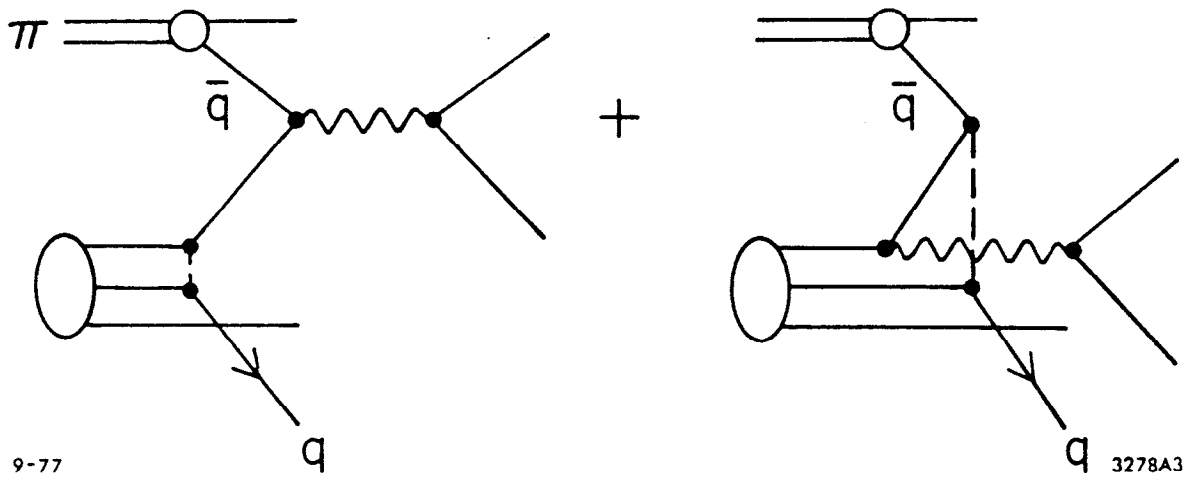
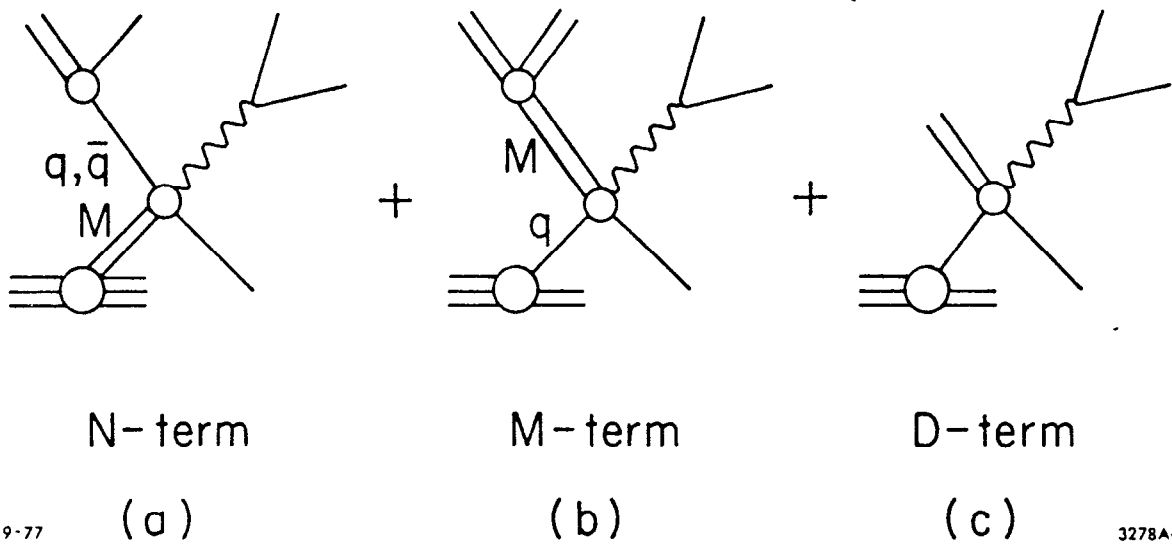


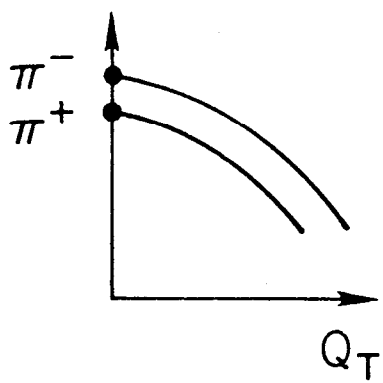
Fig. 4



9-77

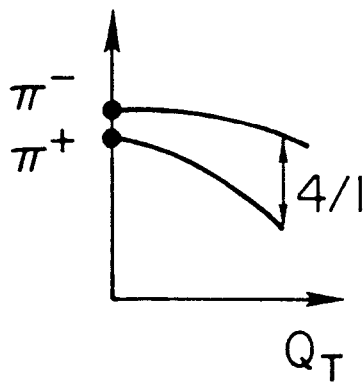
3278A4

Fig. 5



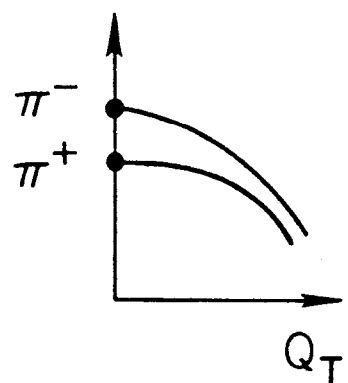
Scattering

(a)



Valence

(b)



Sea

(c)

3278A5

9-77

Fig. 6

$d=1, \mu=0.9$

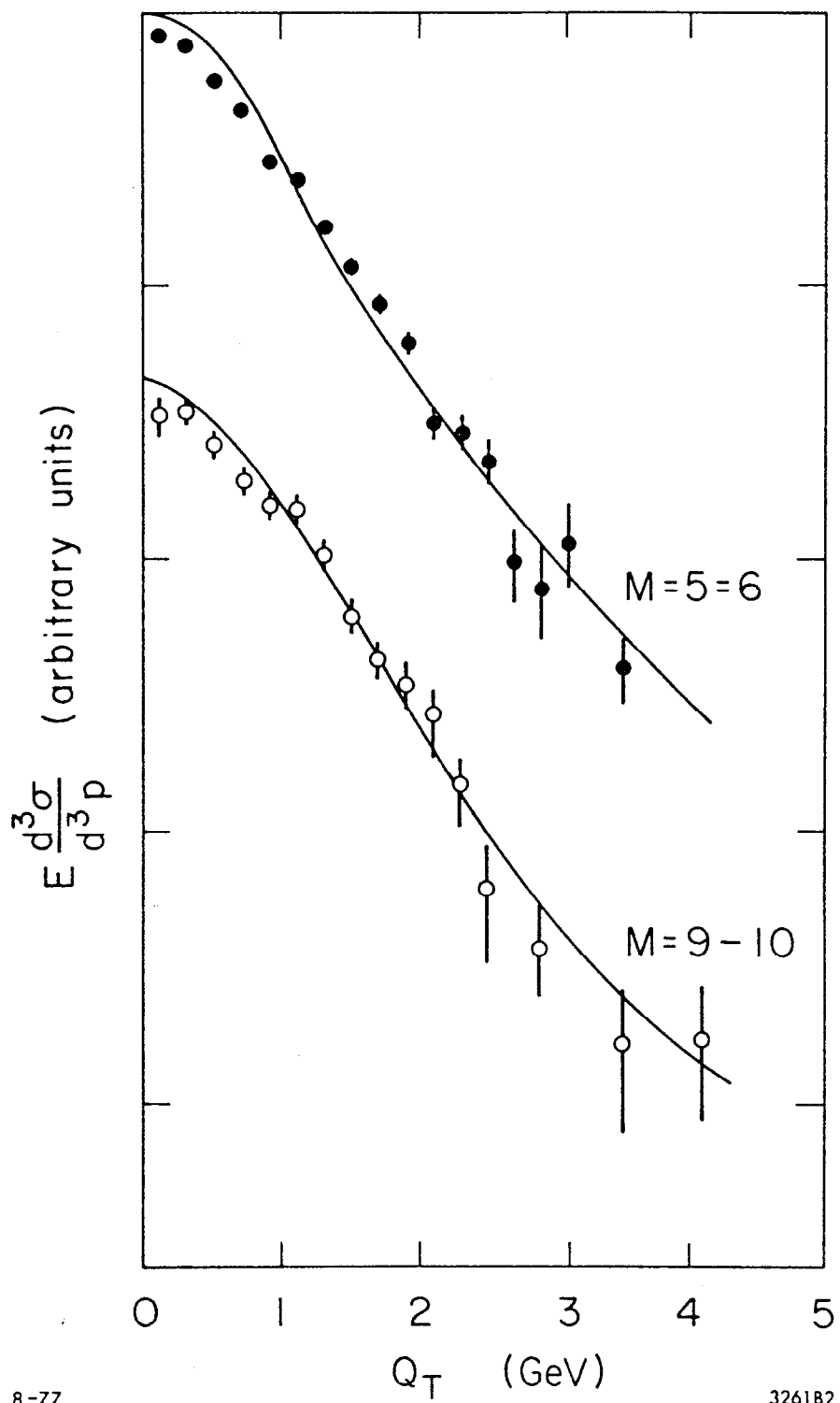


Fig. 7

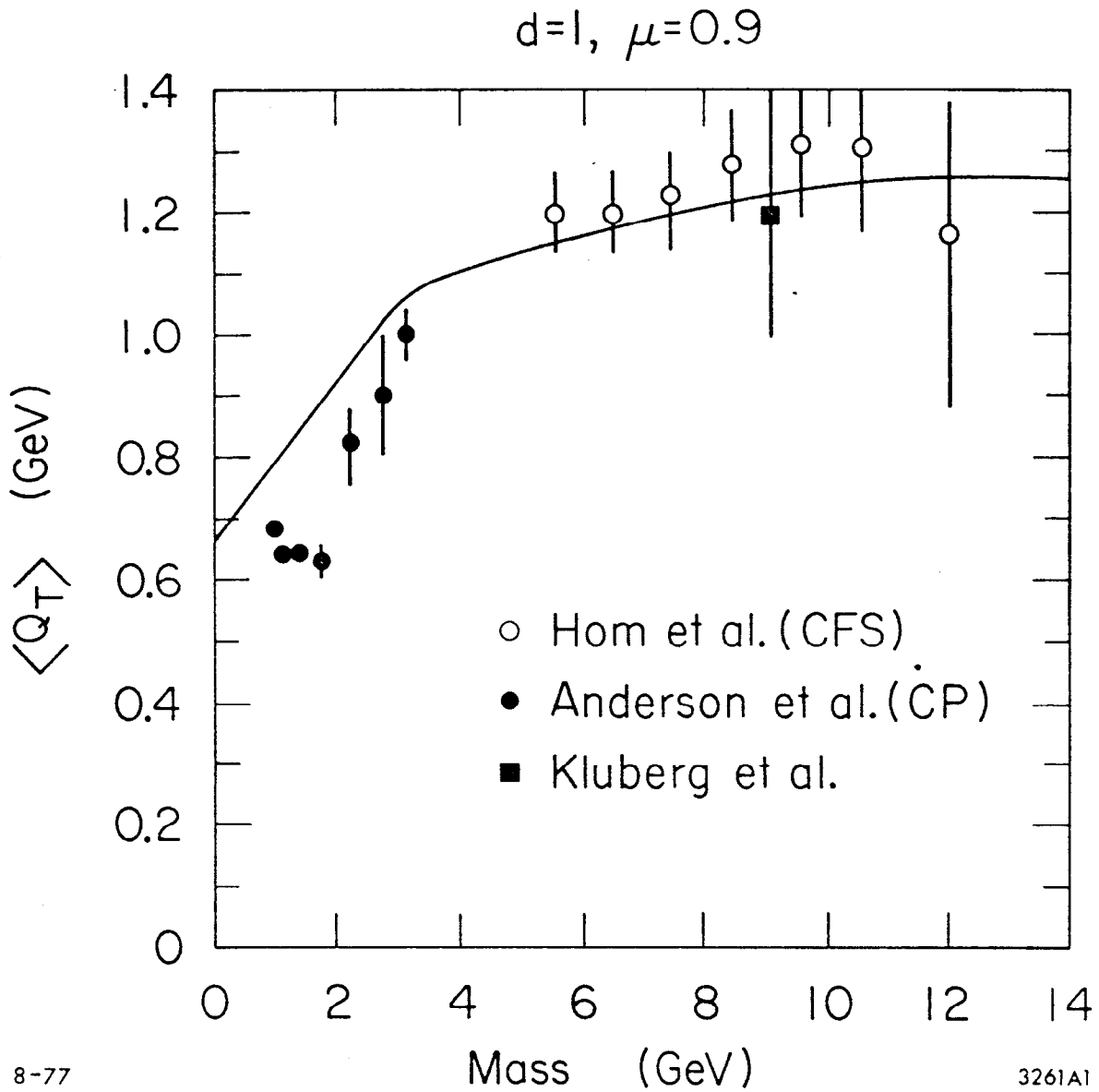


Fig. 8

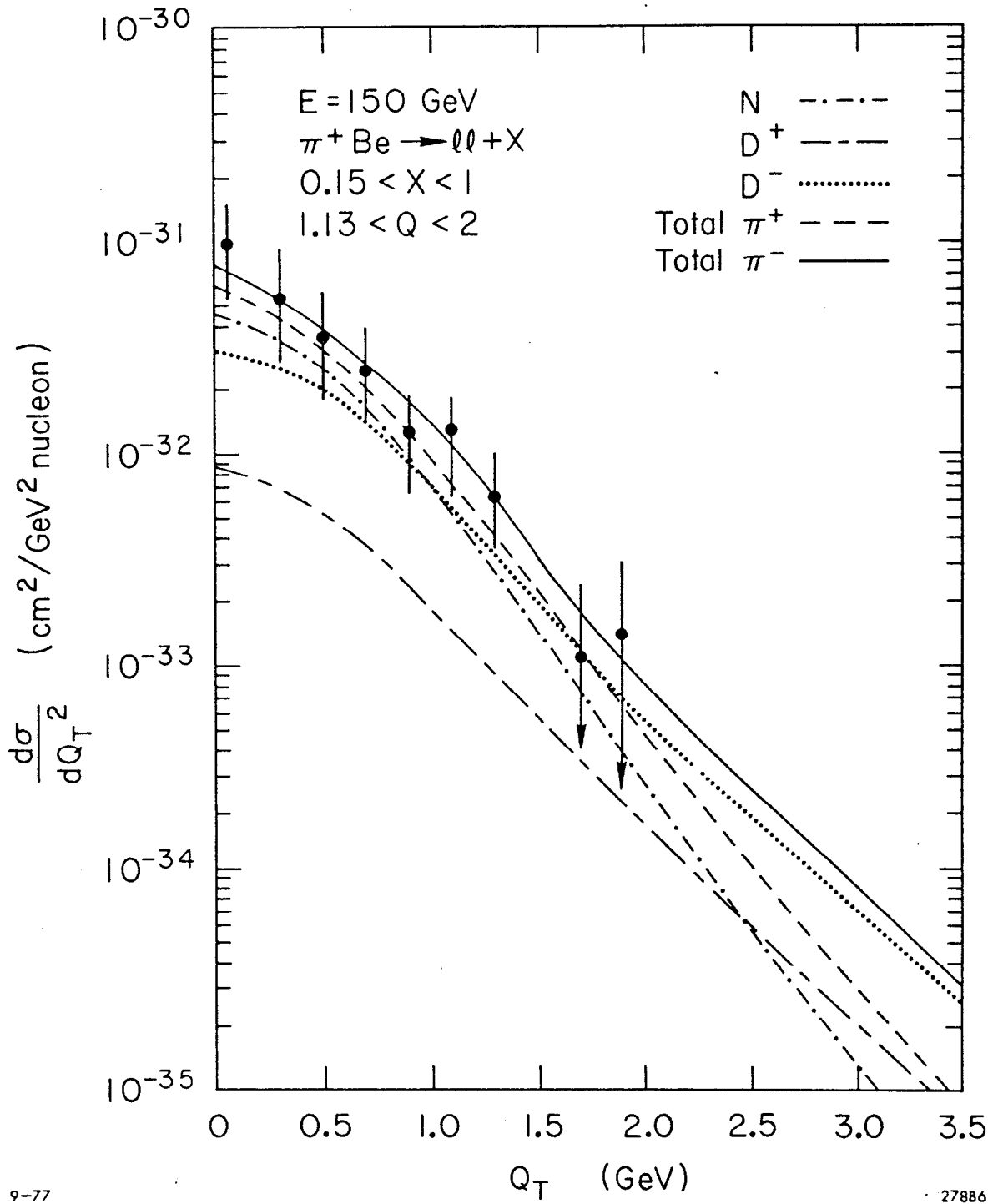


Fig. 9

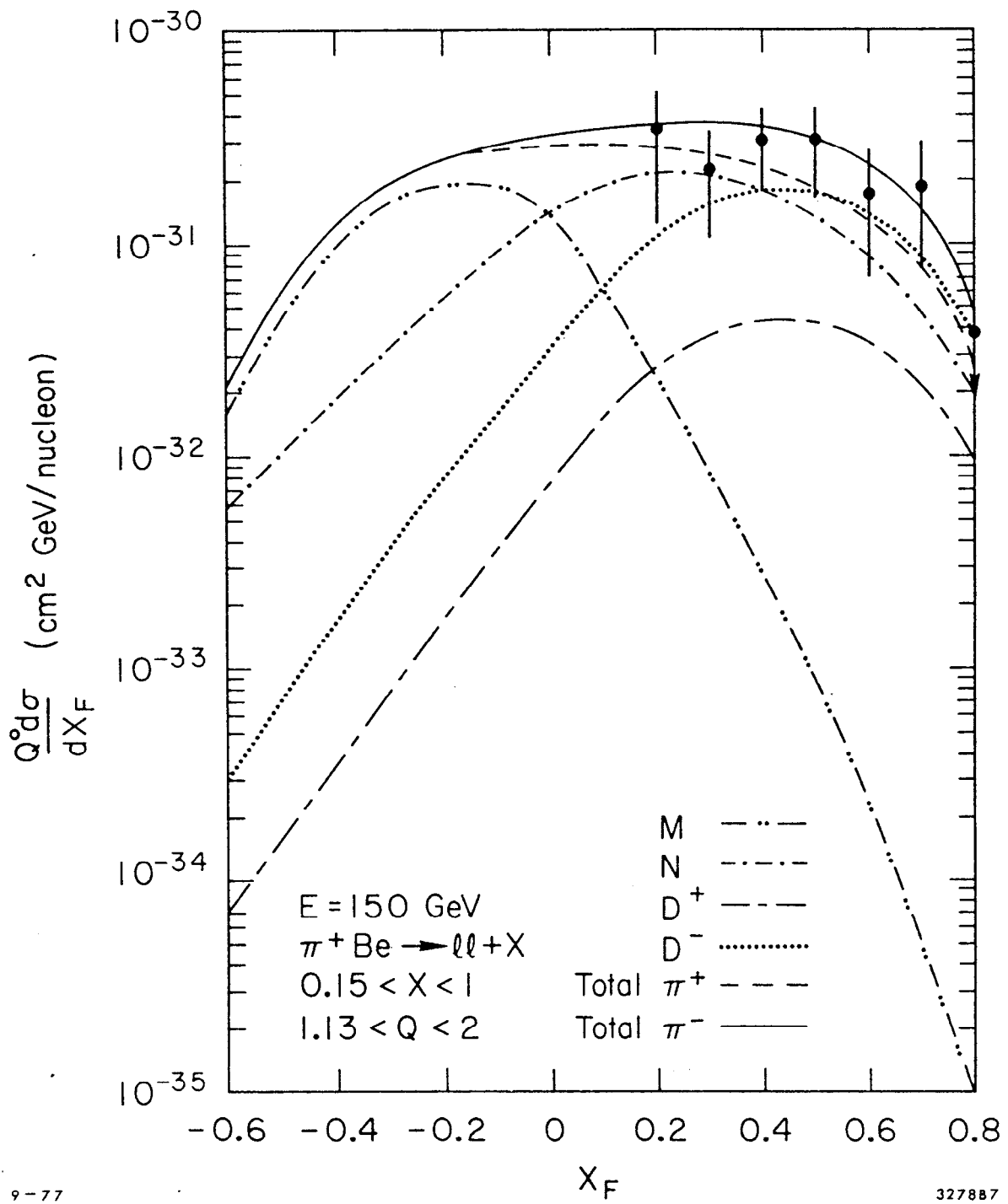


Fig. 10